Simulation of a Wireless Charging Multiple E-Scooters using PV Array with Class-E Inverter Fed by PI Controlled Boost Converter for Constant Output Voltage

Fatih Issi
Electronics and Automation Dept.
Cankiri Karatekin University
Cankiri, Turkey
fatihissi@karatekin.edu.tr

Orhan Kaplan
Electrical and Electronics Engineering Dept.
Gazi University
Ankara, Turkey
okaplan@gazi.edu.tr

***Abstract*— Class-E inverters are high-frequency, high-efficiency inverters with a constant load rating. The load voltage varies when the load resistance at the inverter output changes. As the output load value increases, so does the output voltage. This study generates the inverter input voltage with a solar panel array and enhances it with a boost converter to charge multiple E-Scooters. The output of the boost converter is applied to the input of the Class-E inverter. By running the prepared model at various load values without closed-loop control, it was discovered that the inverter output voltage,which has changed with E-Scooter counts, is variable. In the same circumstance, the inverter power switch has been seen to be in the hard switching condition. The inverter output load voltage is kept constant in the simulation using a PI controller under identical conditions.**

Keywords—Class-E inverter, Constant output voltage, PI Control

I. INTRODUCTION

It is involved in many studies using H-Bridge inverters in high-frequency power supplies[1]. The power loss of each power switch in the H-bridge topology, increasing the total power loss of the system, constitutes the most significant disadvantage[2]. Class-E inverters come into prominence in high-frequency applications due to their low switching losses and 100% theoretical efficiency thanks to their single switch structure, up to a specific power.

High efficiency on power conversion , minimal sensitivity to component variation, and easy circuit architecture and design approaches are made the Class-E inverter ideal for use as a high-frequency inverter. [3]. To avoid excessive current and voltage on the load line and shape the output voltage and current waveform. The switch in Class-E inverters is operated in intermittent mode. [4]. This reduces power loss, particularly during switching transitions. As a result, under constant load Class-E inverters offer considerable benefits due to single switch configuration and reduced switching losses [5]. The most significant shortcoming of Class-E inverters is their inability to keep the constant load voltage at variable loads, requiring the obligatory to regulate load inconstancy[3]. In order to keep the load voltage constant, the need to change the circuit components or control the DC input voltage arises. The DC voltage source for wireless charging applications can be provided by renewable energy sources such as the sun and wind and by rectifying the grid[6].

If the input voltage is supplied from a renewable energy source such as the Solar, the voltage of the solar panel cells decreases as they are loaded[7]. The output voltages of the solar panels can be adjusted by using various converter circuits[7]. When the literature research are analyzed, it is seen that Boost Converters are often preferred to increase the voltage at the solar panel output and make it controllable. Thus, the DC voltage at the solar panels' output is amplified and controlled.

The PI controller is a critical control procedure in closed-loop systems. This technique is commonly utilized in power electronics systems[8-10]. The input signal is compared by the PI control to the output feedback and initiates an error based on the disparity. In response to this error, the PI controller attempts to decrease it and transmits it to the output. In this technique, errors are discovered by giving looping feedback from the output to the input. The method is repeated until the error is decreased to a manageable level. After then, the error is reduced by adding controller effects to the output.

In this study, a simulation study is presented to charge multiple E-Scooters. The simulation study amplifies and controls the DC voltage obtained from solar energy using a Boost converter and controls the obtained voltage using a Class-E inverter input voltage using a PI controller. It is ensured that the load voltage, which has changed with E-Scooter counts, of the different scenarios created for the load change situations at the Class-E inverter output is kept constant. The Block diagram of the model is shown in Fig. 2 and Fig. 2.

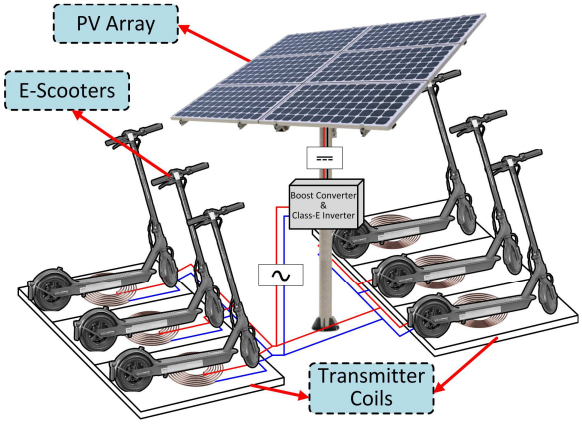

Fig. 1. View of the modeled system

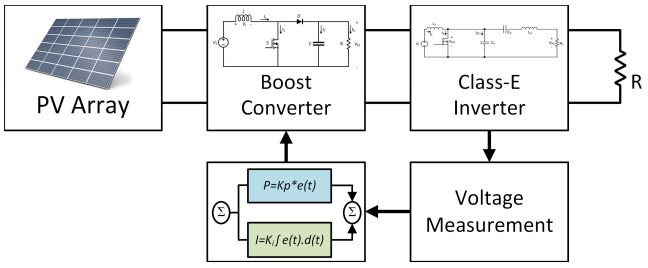

Fig. 2. Block diagram of the modeled system

II. CLASS-E INVERTER

Class-E inverters are high-frequency, high-efficiency soft-switched power converters[11]. Zero-Voltage-Switching (ZVS) and Zero-Derivative-Switching (ZDS) situations occur spontaneously when optimum conditions are met with proper selection of the load value and operation of the output filter in resonance[12, 13]. The efficiency of this inverter topology, which has 100% theoretical efficiency under constant load, decreases due to reasons such as the disappearance of the ZVS condition under variable load and the failure to meet the inverter output resonance condition[14]. Disruption of the ZVS condition causes high switching losses and reduces the inverter efficiency[15, 16]. Fig. 3 shows the circuit topology of the Class-E inverter.

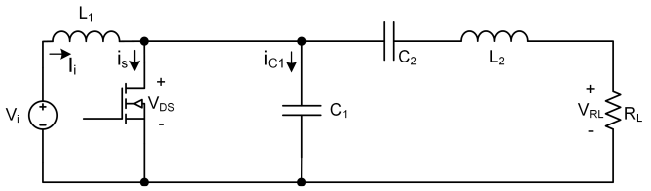

Fig. 3. Circuit topology of the Class-E inverter

At the optimum load resistance value, the inverter's optimal operating point is attainable only. [17]. When the load resistance exceeds the ideal, the peak current through the resonant circuit is less than the current required for optimum operation.

When the switch is conducted, the voltage on the capacitor C_1 and switch becomes v_s=0. When the switch is in the cutoff position, the voltage of the C_1 capacitor is computed as shown in (1).

$$v_s = \frac{1}{\omega C_1}\int_{2\pi D}^{\omega t} i_{C1}\, d(\omega t) \tag{1}$$

(2) presents the solution of the problem based on time intervals.;

$$v_s = \begin{cases} 0 & , \quad 0 < \omega t \le 2\pi D \\ \frac{1}{\omega C_1} + (I_{in}(\omega t - 2\pi D) + & , \quad 2\pi D < \omega t \le 2\pi \\ I_m \cos(\omega t + \varphi) - \cos(2\pi D + \varphi) & \end{cases} \tag{2}$$

(3) expresses the total current taken from the source as a function of input voltage and load resistance.

$$I_1 = \frac{8}{\pi^2 + 4}\frac{V_s}{R_L} \tag{3}$$

It has been emphasized that E-class inverters are ideal for high-frequency applications, but they have a few disadvantages. It has been evaluated that the most important of these disadvantages is that the voltage stress that may occur on the power switch can increase up to 3.5 times. It becomes difficult to use this inverter under variable load conditions, and the efficiency varies a lot[18]. In Fig. 4.(a), the voltage and current waveforms of the power switch are given for the cases where the inverter is at the optimum operating point, below the optimum operating point in (b) and above it in (c).

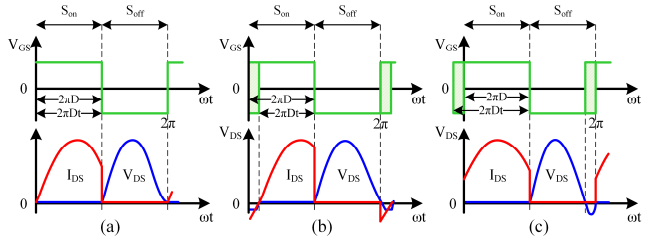

Fig. 4. Voltage and current waveforms of the Class-E inverter at; a) optimum operation, b) suboptimum operation, c)non-optimum operation

In Fig. 4.(a) and (b) soft switching occurs, (c) occurs with hard switching. In hard switching, the inverter efficiency decreases considerably.

III. PV ARRAY AND BOOST CONVERTER

A. PV Array

In the simulation study, a solar panel array consisting of 4 series-10parallel strings with open circuit voltage V_{oc}=44V and short circuit voltage I_{sc}=5.17A was used. The output voltage of the panel array is adjusted to be approximately 192V.

B. Boost Converter

Boost converters are power converters in Fig. 5. where the output voltage is always greater than the input voltage. The converter consists of the DC input voltage source V_S, the boost inductor L, the controlled switch S, the diode D, the filter capacitor C, and the load resistor R[19].

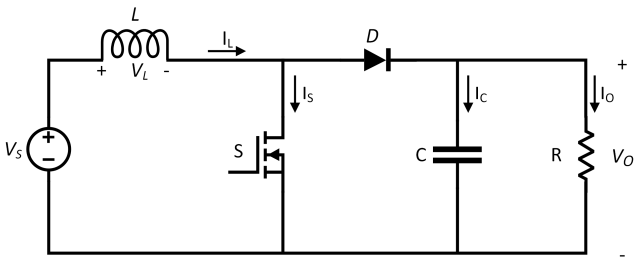

Fig. 5. Circuit topology of the Boost Converter

With switch S open in the converter, the current in the boost inductor rises in a linear fashion. At the moment, diode D is turned off. When the switch S is switched off, the inductor's stored energy is released to the input RC circuit through the diode[20]. Using Faraday's law to design a boost inductor,

$$V_S DT = (V_O - V_S)(1 - D)T \tag{4}$$

which the dc voltage transfer function is determined to be

$$\frac{V_O}{V_S} = \frac{1}{1 - D} \tag{5}$$

For L> L_b, the boost converter works in the Continuous Conduction Mode,

$$L_b = \frac{(1-D)^2 DR}{2f} \quad (6)$$

The current provided to the output RC circuit is discontinuous, as shown in Fig. 6.

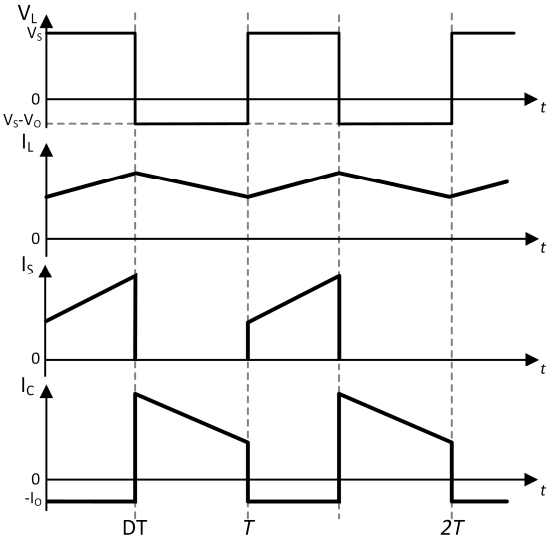

Fig. 6. Continuous Current Mode voltage-current waveforms of Boost Converter

As a result, a bigger filter capacitor is required to minimize the output voltage ripple than in buck-derived converters. When diode D is turned off, the filter capacitor must supply the output dc current to the load. V_r is the minimal value of the filter capacitance that results in voltage ripple.

$$C_{min} = \frac{DV_o}{V_r Rf} \quad (7)$$

C. PI Controller

One of the most important control processes in closed-loop and control systems is the PI controller. This technique is commonly applied in power electronics systems[19]. The mathematical model for PI control, which is a linear control approach, is provided in (8). Here, K_p and K_i indicate proportional and integral gain, respectively, *F(t)* stands for the control signal, and *e* stands for error[21, 22].

$$F(t) = K_p e(t) + K_i \int e(t) d(t) \quad (8)$$

The PI control compares the input signal to the output feedback and generates an error based on the difference between these two signals. The PI controller responds to this error by attempting to reduce it and passing it to the output. Errors are recognized in this manner by continual feedback from the output to the input. The procedure is repeated until the error is reduced. The error is then decreased by applying controller effects to the output. Because the mathematical model is simple and the number of adjustment parameters to be altered is limited, this control approach is highly recommended[22, 23].

IV. SIMULATION

The model consisting of a solar panel array, boost converter, and Class-E inverter was modeled using Matlab/Simulink and presented in Fig. 7.

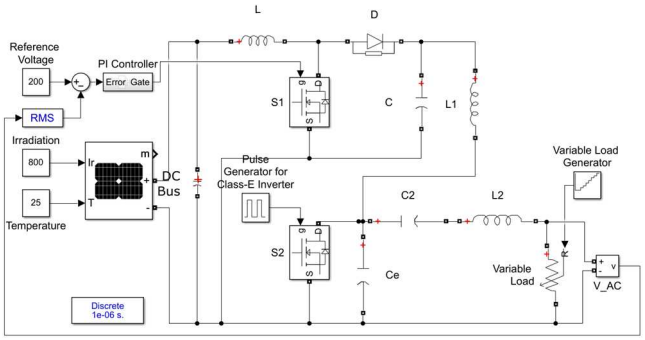

Fig. 7. Prepared model on Simulink

In the model, the solar array is provided to produce DC bus voltage under constant solar radiation and panel temperature. The obtained DC bus voltage is applied to the Boost converter input. The DC voltage obtained at the boost converter output is applied to the Class-E inverter input. Class-E inverter has a switching frequency of 85kHz and the optimum load value is designed as 50Ω. It was increased by 25 Ω steps in the range of 25-150 Ω, respectively, for the change of the load value. As a result of operating the boost converter with a fixed switching ratio in the system, the inverter output load voltage was monitored. It has been observed that the output voltage increases as the inverter output load resistance increases. Under these conditions, V_{DS} and I_{DS} waveforms of Class-E inverter were also obtained. Output load voltage graph and waveforms of power switch voltage and current obtained when Class-E inverter operates without PI controller are presented in Fig. 8. and Fig. 9.(a)-(f).

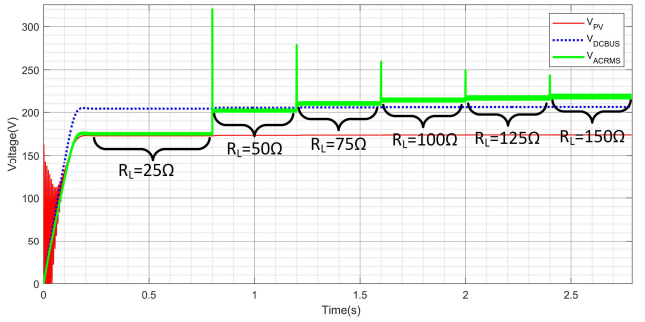

Fig. 8. Output load voltage without PI Controller

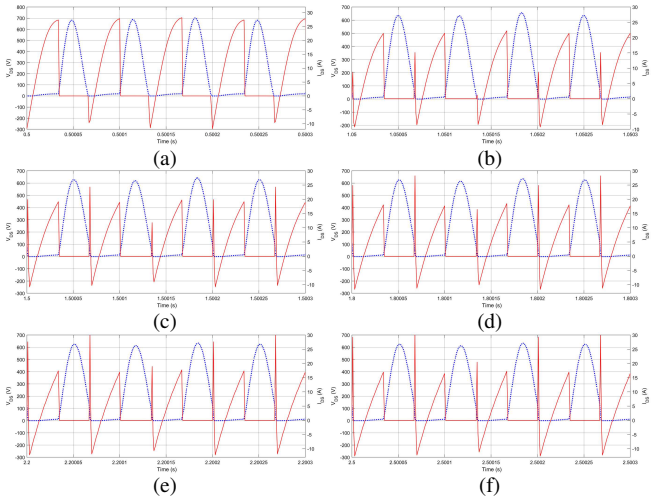

Fig. 9. Power switch voltage and current waveforms without PI Controller; a) R_L=25Ω, b) R_L=50Ω, c) R_L=75Ω, d) R_L=100Ω, e)R_L=125Ω, f) R_L=150Ω.

When the V_{DS} and I_{DS} graphics of the power switch are examined, the optimum-suboptimum conditions presented in Fig. 9.(a) and (b) for 25 Ω and 50 Ω load values have been realized and the power switch is operating under ZVS conditions. For load values of 75 Ω and above, the inverter has entered the hard switching zone. In the case of hard switching, the switching losses increase.

The inverter was operated under the same load conditions using a PI controller. The variation of the inverter load voltage and the voltage-current graphs of the inverter are presented in Fig. 10. and Fig. 11(a)-(f). It has been observed that the PI controller keeps the inverter output voltage constant at 200V RMS. When the voltage-current graphs of the power switch are examined, it is observed that the inverter operates under suboptimal conditions.

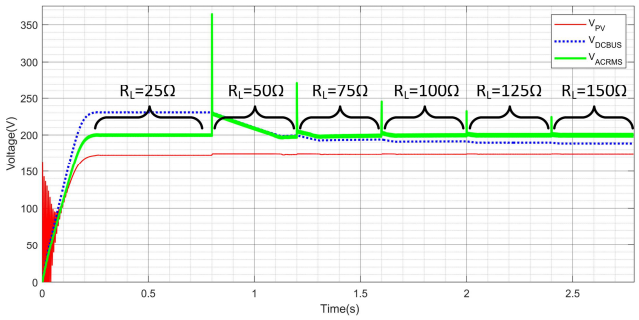

Fig. 10. Output load voltage with PI Controller

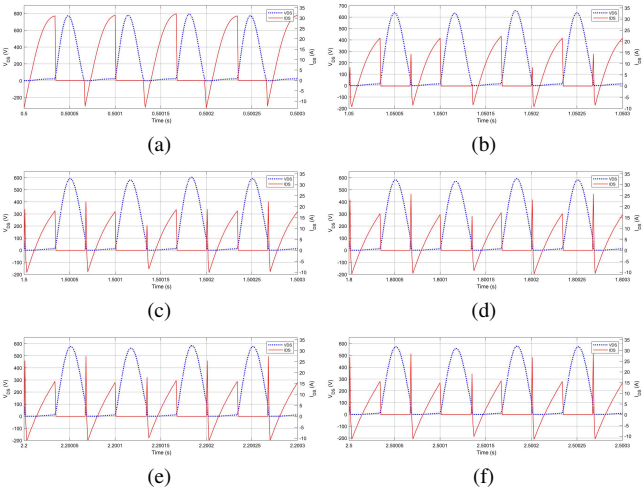

Fig. 11. Power switch voltage and current waveforms with PI Controller; a) R_L=25Ω, b) R_L=50Ω, c) R_L=75Ω, d) R_L=100Ω, e)R_L=125Ω, f) R_L=150Ω.

V. Results

Class-E inverters are high-frequency inverters with high efficiency for constant load rating. If the load resistance at the inverter output changes, the load voltage changes. As the output load value increases, the output voltage also increases. In this study, the inverter input voltage is generated with a solar panel array and increased using a boost converter. The boost converter output voltage is applied to the Class-E inverter input. It has been observed that the inverter output voltage is variable by operating the prepared model at variable load values without closed-loop control. In the same situation, it has been observed that the inverter power switch is in the hard switching state. In the simulation using a PI controller under the same conditions, the inverter output load voltage is kept constant. The prepared simulation study can also be run in variable solar radiation and panel temperatures.

References

[1] L. He and D. Guo, "Compound Voltage Clamped Class-E Converter With ZVS and Flexible Power Transfer for WPT System," IEEE Transactions on Power Electronics, vol. 35, no. 7, pp. 7123-7133, 2020, doi: 10.1109/TPEL.2019.2954078.

[2] O. C. Onar, M. Chinthavali, S. Campbell, P. Ning, C. P. White, and J. M. Miller, "A SiC MOSFET based inverter for wireless power transfer applications," in 2014 IEEE Applied Power Electronics Conference and Exposition - APEC 2014, Fort Worth, Texas, USA, 16-20 March 2014 2014, pp. 1690-1696, doi: 10.1109/APEC.2014.6803533.

[3] S. Li, W. Li, J. Deng, T. D. Nguyen, and C. C. Mi, "A Double-Sided LCC Compensation Network and Its Tuning Method for Wireless Power Transfer," IEEE Transactions on Vehicular Technology, vol. 64, no. 6, pp. 2261-2273, 2015, doi: 10.1109/TVT.2014.2347006.

[4] Z. Pantic, S. Bai, and S. M. Lukic, "ZCS LCC-Compensated Resonant Inverter for Inductive-Power-Transfer Application," IEEE Transactions on Industrial Electronics, vol. 58, no. 8, pp. 3500-3510, 2011, doi: 10.1109/TIE.2010.2081954.

[5] S. Samanta and A. K. Rathore, "A New Current-Fed CLC Transmitter and LC Receiver Topology for Inductive Wireless Power Transfer Application: Analysis, Design, and Experimental Results," IEEE Transactions on Transportation Electrification, vol. 1, no. 4, pp. 357-368, 2015, doi: 10.1109/TTE.2015.2480536.

[6] P. Geetha and S. Usha, "Critical Review and Analysis of Solar Powered Electric Vehicle Charging Station," International Journal of Renewable Energy Research, vol. 12, no. 1, pp. 581-600, 2022.

[7] J. Tian and A. P. Hu, "A DC-Voltage-Controlled Variable Capacitor for Stabilizing the ZVS Frequency of a Resonant Converter for Wireless Power Transfer," IEEE Transactions on Power Electronics, vol. 32, no. 3, pp. 2312-2318, 2017, doi: 10.1109/TPEL.2016.2559798.

[8] X. Liu, J. Liu, J. Wang, C. Wang, and X. Yuan, "Design Method for the Coil-System and the Soft Switching Technology for High-Frequency and High-Efficiency Wireless Power Transfer Systems," Energies, vol. 11, no. 1, p. 7, 2018.

[9] I. Setiawan, M. Facta, A. Priyadi, and M. H. Purnomo, "Investigation of symmetrical optimum PI controller based on plant and feedback linearization in Grid-Tie inverter systems," International Journal of Renewable Energy Research, vol. 7, no. 3, pp. 1228-1234, 2017.

[10] A. Mamizadeh, N. Genc, and R. Rajabioun, "Optimal Tuning of PI Controller for Boost DC-DC Converters Based on Cuckoo Optimization Algorithm," in 2018 7th International Conference on Renewable Energy Research and Applications (ICRERA), 14-17 Oct. 2018 2018, pp. 677-680, doi: 10.1109/ICRERA.2018.8566883.

[11] R. Zulinski, "A high-efficiency self-regulated class E power inverter/converter," IEEE transactions on industrial electronics, vol. 33, no. 3, pp. 340-342, 1986.

[12] N. O. Sokal, "Class-E RF Power Amplifiers," 2001.

[13] A. Kiri, M. Sato, S. Kuga, W. Xiuqin, and T. Suetsugu, "Power dissipation at MOSFET gate port of class E amplifier," in 2013 International Conference on Renewable Energy Research and Applications (ICRERA), 20-23 Oct. 2013 2013, pp. 326-329, doi: 10.1109/ICRERA.2013.6749774.

[14] F. Raab, "Idealized operation of the class E tuned power amplifier," IEEE Transactions on Circuits and Systems, vol. 24, no. 12, pp. 725-735, 1977, doi: 10.1109/TCS.1977.1084296.

[15] A. Lotfi et al., "Subnominal Operation of Class-E Nonlinear Shunt Capacitance Power Amplifier at Any Duty Ratio and Grading Coefficient," IEEE Transactions on Industrial Electronics, vol. 65, no. 10, pp. 7878-7887, 2018, doi: 10.1109/TIE.2018.2803767.

[16] Y. Komiyama, W. Zhu, K. Nguyen, and H. Sekiya, "Class-E Inverter with Frequency Modulation Control," in 2021 10th International Conference on Renewable Energy Research and Application (ICRERA), 26-29 Sept. 2021 2021, pp. 94-98, doi: 10.1109/ICRERA52334.2021.9598543.

[17] M. K. Kazimierczuk, RF Power Amplifiers. Wiley, 2008.

[18] C. L. Espinosa, "Asynchronous non-inverter buck-boost DC to DC converter for battery charging in a solar MPPT system," in 2017 IEEE URUCON, 23-25 Oct. 2017 2017, pp. 1-4, doi: 10.1109/URUCON.2017.8171863.

[19] R. Sharma, N. Goel, and S. Chacko, "Performance Investigation of Fractional PI Controller in Shunt Active Filter for a Three Phase Four Wire System," in 2018 4th International Conference on Computing Communication and Automation (ICCCA), 14-15 Dec. 2018 2018, pp. 1-7, doi: 10.1109/CCAA.2018.8777576.

[20] D. Czarkowski, "13 - DC–DC Converters," in Power Electronics Handbook (Third Edition), M. H. Rashid Ed. Boston: Butterworth-Heinemann, 2011, pp. 249-263.

[21] S. Reimann, W. Wu, and S. Liu, "Real-Time Scheduling of PI Control Tasks," IEEE Transactions on Control Systems Technology, vol. 24, no. 3, pp. 1118-1125, 2016, doi: 10.1109/TCST.2015.2464304.

[22] S. Vadi, F. B. Gurbuz, S. Sagiroglu, and R. Bayindir, "Optimization of PI Based Buck-Boost Converter by Particle Swarm Optimization Algorithm," in 2021 9th International Conference on Smart Grid (icSmartGrid), 29 June-1 July 2021 2021, pp. 295-301, doi: 10.1109/icSmartGrid52357.2021.9551229.

[23] R. Das, H. Rashid, and I. U. Ahmed, "A comparative analysis of PI and PID controlled bidirectional DC-DC converter with conventional bidirectional DC-DC converter," in 2017 3rd International Conference on Electrical Information and Communication Technology (EICT), 7-9 Dec. 2017 2017, pp. 1-6, doi: 10.1109/EICT.2017.8275149.